DINAME 2019 - Proceedings of the XVIII International Symposium on Dynamic Problems of Mechanics,
M.A. Savi, T.G. Ritto and W.M. Bessa (Editors), ABCM, Buzios, RJ, Brazil, March 10th to 15th, 2019

Torque Optimization for Stability Control for Wheeled Vehicles in Rough Terrain

Vivian Suzano Medeiros, Diego Gabriel Gomes Rosa and Marco Antonio Meggiolaro

Pontifical Catholic University of Rio de Janeiro, Rua Marquês de São Vicente, 225, Gávea, Rio de Janeiro, 22453-900, RJ, Brasil, viviansuzano@puc-rio.br, diegorosa@aluno.puc-rio.br, meggi@puc-rio.br

Abstract: This paper aims at improving dynamical stabilization of wheeled robots moving in rough terrain. Two algorithms are used to obtain the optimal torque values at each vehicle wheel for trajectories in terrains with different levels of difficulty: the interior-point method and an evolutionary algorithm. The algorithms are evaluated through simulations based on the dynamic equations of movement and from experimental tests. With these techniques, it is possible to evaluate the behavior and the limitations of a mobile robot in extreme stability conditions. This practice is useful to guarantee the safety of the equipment in highly uneven terrains, with applications in inspection and rescue mobile robots.

Keywords: torque optimization, stability control, mobile robots, rough terrain

INTRODUCTION

Unmanned ground vehicles constitute a research field that is rising rapidly. Military, industrial, agricultural, spatial and even humanitarian tasks are some applications of these machines (Rasam, 2016; Michaud et al., 2008; Khamis, 2016). The state of art in this area normally includes studies about navigation algorithms, vision systems or artificial intelligence as the most necessary developments for autonomous vehicles and mobile robot applications (Jin et al., 2018). However, the development of these vehicles depends on diverse factors, such as the system dynamical characteristics and the interactions with its environment (Caltabiano, 2004; Stückler et al., 2016). In this work, the mechanical stability and control are studied according to terrain physical and geometrical characteristics.

To solve real world problems, different solutions appear. Hamid et al. (2016) developed a locomotion system based on mechanical design optimization, verifying that a six-wheeled robot has mechanical advantages when used in rough terrains. Iagnemma et al. (2000) performed similar work, by producing a wheeled system with reconfigurable design for improved stability. Iagnemma and Dubowsky (2004) also identified that, as the mechanical design has a great importance, the dynamics of the movement should not be neglected, while traction control can provide improvements on the stability problem. Silva et al. (2010) developed a traction control technique based on friction and normal forces, to guarantee the dynamic stability and to avoid wheel slippage in previously known terrains. They used a graphical analysis to examine planar movements and provide a closed form solution for the optimal independent wheel torques. However, the method used by them does not provide a closed-form solution for 3D cases. Mazulina et al. (2016) adopted a set of sensors to predict the terrain characteristics in situ, but only for 2D movements. The 3D analyses are usually performed with grid maps. In this case, LIDAR or stereo vision cameras can be used to generate the map. However, the precision of this technique is low and usually data is used only to avoid high depressions or obstacles (Stückler et al., 2016).

This work presents a method to generalize traction control, with an algorithm that can be useful in 3D cases. It is valid for wheeled robots with any number of wheels, applicable to the case where the terrain shape is unknown and an obstacle has to be exceeded. Two algorithms are presented to solve the problem: the first one based on a gradient evaluation optimization algorithm and the second one using genetic algorithms multi-objective optimization.

VEHICLE MODELING

This section introduces the modeling and kinematic analysis for a vehicle moving on rough terrain, considering initially a two-dimensional approach. The chassis and the wheels are considered as a rigid body, and the mass of the system is concentrated at the center of mass of the chassis. The 2D modeling is important for inferring stability metrics for the vehicle both on the longitudinal axis and on the transverse axis in different conditions, such as acceleration/deceleration in stationary condition or quasi-static condition. The model is built under the following hypotheses: the wheel and the soil do not deform; the contact between the wheel and the ground occurs at a single point, which is reasonable for rigid (non-deformable) wheels; the contact angles between each wheel and the ground are allowed to be different; and the friction coefficient of the soil is known or can be estimated. Figure 1 illustrates the forces acting on the vehicle on rough terrain, in two dimensions.

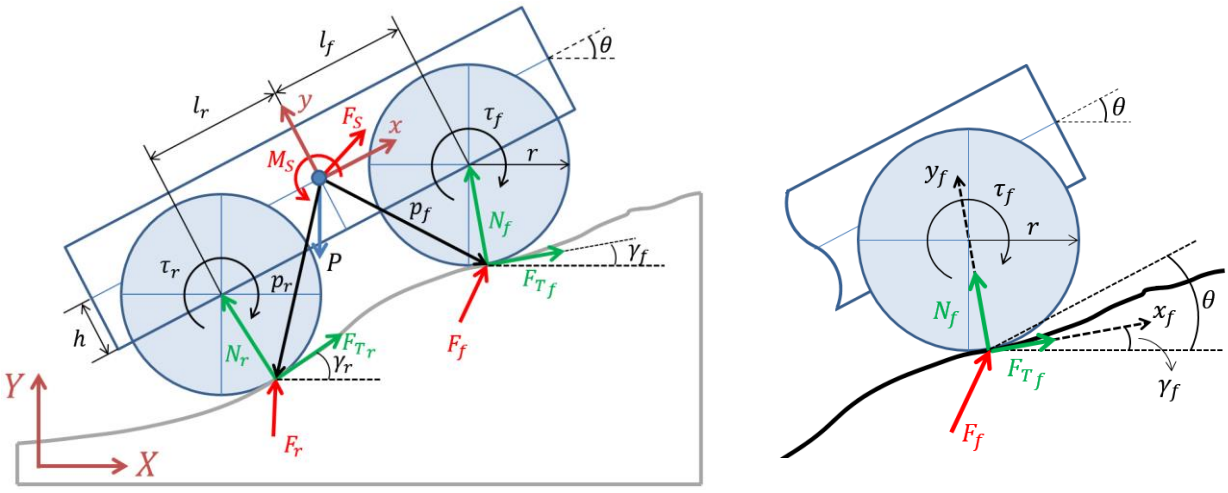

(a) **(b)**

Figure 1 – Forces acting on the vehicle on rough terrain.

Throughout the equations, the subscripts f and r indicate variables corresponding to the front and rear wheels, respectively. As it can be seen in Fig. 1, the traction forces in the wheels are designated as $\mathbf{F_T}$, the normal forces on the wheels are represented by **N** and the torques at the wheels generated by the motors by τ. The contact angles between each wheel and the ground are referenced by γ, while the angle θ represents the inclination of the vehicle chassis. The known parameters of the vehicle are: the wheel radius r, half of the height of the chassis h, the mass m of the chassis + wheels, the moment of inertia J_z of the vehicle with respect to the axis z, and the distances between the wheels axis and the center of mass of vehicle, denominated as l_f and l_r. {X,Y}is the global reference and the {x, y} is the local reference, positioned at the center of mass of the system.

First, consider a coordinate system $\{x_i, y_i\}$ located from the point of contact between the wheel and the ground, as shown in Fig. 1b. The contact forces $\mathbf{F_r}$ (rear wheel) and $\mathbf{F_f}$ (front wheel) can then be decomposed into a normal force $\mathbf{N_i}$ and a tangential force $\mathbf{F_{T_i}}$ (traction force). In the wheels reference axis, the forces $\mathbf{F_r}$ and $\mathbf{F_f}$ can be described as:

$$\mathbf{F_f} = \begin{bmatrix} F_{T_f} \\ N_f \end{bmatrix} \quad \text{e} \quad \mathbf{F_r} = \begin{bmatrix} F_{T_r} \\ N_r \end{bmatrix} \tag{1}$$

In order to determine the forces $\mathbf{F_S}$ and $\mathbf{M_S}$ acting on the center of mass of the vehicle**,** the contact forces on the wheels need to be defined in the coordinate system solidary to the chassis {x, y}. For this, it is possible to define the following rotation matrices:

$$\mathbf{R_f} = \begin{bmatrix} \cos(\theta - \gamma_f) & -\sin(\theta - \gamma_f) \\ \sin(\theta - \gamma_f) & \cos(\theta - \gamma_f) \end{bmatrix}, \quad \mathbf{R_r} = \begin{bmatrix} \cos(\theta - \gamma_r) & -\sin(\theta - \gamma_r) \\ \sin(\theta - \gamma_r) & \cos(\theta - \gamma_r) \end{bmatrix} \tag{2}$$

The vectors $\mathbf{p_d}$ and $\mathbf{p_t}$ represent the distances between the center of mass of the vehicle and the points of contact in the wheels written in the local reference frame {x, y}, given by:

$$\mathbf{p_f} = \begin{bmatrix} l_f - r\sin(\theta - \gamma_f) \\ -(h + r\cos(\theta - \gamma_f)) \end{bmatrix} = \begin{bmatrix} p_{f_x} \\ p_{f_y} \end{bmatrix}, \quad \mathbf{p_r} = \begin{bmatrix} -(l_r + r\sin(\theta - \gamma_r)) \\ -(h + r\cos(\theta - \gamma_r)) \end{bmatrix} = \begin{bmatrix} p_{r_x} \\ p_{r_y} \end{bmatrix} \tag{3}$$

Then, total force $\mathbf{F_S}$ and the total moment $\mathbf{M_S}$ are determined by:

$$\begin{bmatrix} \mathbf{F_S} \\ \mathbf{M_S} \end{bmatrix} = \begin{bmatrix} F_{S_x} \\ F_{S_y} \\ M_z \end{bmatrix} = \begin{bmatrix} \mathbf{R_f} & \mathbf{R_r} \\ [p_{f_y} \quad -p_{f_x}]\mathbf{R_d} & [p_{r_y} \quad -p_{r_x}]\mathbf{R_t} \end{bmatrix} \begin{bmatrix} \mathbf{F_f} \\ \mathbf{F_r} \end{bmatrix} \tag{4}$$

They can also be defined as a function of the acceleration on each axis:

$$\begin{aligned} F_{S_x} - mg\sin\theta &= m\,\ddot{x} \\ F_{S_y} - mg\cos\theta &= m\,\ddot{y} \\ M_z &= J_z\,\ddot{\theta} \end{aligned} \tag{5}$$

Applying (5) in (4), the equations of motion are obtained:

$$\begin{bmatrix} m\,\ddot{x} \\ m\,\ddot{y} \\ J_z\ddot{\theta} \end{bmatrix} = \begin{bmatrix} & \mathbf{R_f} & & \mathbf{R_r} \\ [p_{f_y} & -p_{f_x}]\mathbf{R_d} & [p_{r_y} & -p_{r_x}]\mathbf{R_t} \end{bmatrix} \begin{bmatrix} F_{T_f} \\ N_f \\ F_{T_r} \\ N_r \end{bmatrix} + \begin{bmatrix} -mg\sin\theta \\ -mg\cos\theta \\ 0 \end{bmatrix} \tag{6}$$

Here it is important to notice the importance of knowing the inclination angle of the chassis and the contact angles between the wheels and the ground for the simulation of the system. In the experimental vehicle, this data can be obtained from the onboard instrumentation in the vehicle and the wheels, as proposed by Iagnemma and Dubowsky (2004), Lamon and Siegwart (2005) and Xu et al. (2014).

TORQUE OPTIMIZATION

For robotic vehicles to be able to move safely on highly rough terrain, it is necessary to implement a wheel traction control that is capable of guaranteeing the stability of the vehicle in hazardous situations. However, the set of torques to be applied on the wheels cannot be determined uniquely, as there are several possible configurations that would lead to the stability of the vehicle. Therefore, a multi-objective optimization will be implemented to determine ideal torques to be applied on the wheels under different conditions. The optimization criteria can be numerous: maintain vehicle stability (avoid tipping and loss of wheel contact with the ground), prevent engine saturation, reduce power consumption, maximize traction and prevent wheel slippage.

Tipover Stability Measure

Papadopoulos and Rey (2000) proposed a criterion for the static and dynamic stability of a vehicle based on measures of forces and angles, called the Force-Angle Stability Measure. Consider the vehicle shown in Figure 2, the stability measure α is given by the minimum of the two angles β_f and β_r weighted by the magnitude of the total force acting on the vehicle's center of mass. In the case on the figure, it would be $\alpha = \beta_f \|\mathbf{f}\|$.

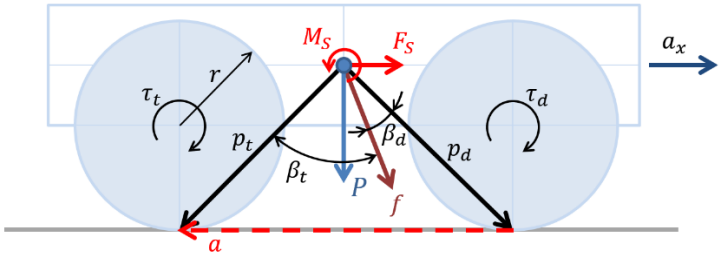

Figure 2 – Example of stability measure.

The distance between the vehicle's center of mass and each wheel-ground contact points are represented by the vectors $\mathbf{p_f}$ and $\mathbf{p_r}$, defined in Eq. (3). The tipover angles β_f and β_r and the tipover stability measure α are given by:

$$\begin{aligned} \beta_{f,r} &= \cos^{-1}\left(\hat{\mathbf{f}} \cdot \hat{\mathbf{p}}_{\mathbf{f,r}}\right) \\ \alpha &= \|\mathbf{f}\| \min(\beta_f, \beta_r) \end{aligned} \tag{7}$$

where $\hat{\mathbf{v}} = \mathbf{v}/\|\mathbf{v}\|$, for a given vector $\mathbf{v}$. The force $\mathbf{f}$ consists in the sum of all forces acting on the vehicle body, making it necessary to replace the moment $\mathbf{M_S}$ with an equivalent force couple $\mathbf{f_m}$. There are infinite force couples that would cause the same moment, however it is interesting to determine the pair where one member of the couple passes through the center of mass and the other through the tipover axis $\boldsymbol{a}$. The force couple acting on the center of mass can be obtained by the following equation:

$$\begin{aligned} \mathbf{f_m} &= \frac{\hat{\mathbf{l}} \times \mathbf{M_S}}{\|\mathbf{l}\|}, \text{where } \mathbf{l} = (\mathbf{I} - \hat{\boldsymbol{a}}\hat{\boldsymbol{a}}^T)\mathbf{p_t} \\ \mathbf{f} &= \mathbf{F_S} + \mathbf{P} + \mathbf{f_m} \end{aligned} \tag{8}$$

where $\mathbf{I}$ is the identity matrix.

Note that when $\alpha = 0$, the force $\mathbf{f}$ coincides with either $\mathbf{p_f}$ or $\mathbf{p_r}$ and the vehicle is in the imminence of tipping over. When $\alpha < 0$, the vehicle is already in a tipover condition. That is why it is desirable that the value of α remains large and positive, to maintain the vehicle in the stability region.

Optimization Problem and Matlab Simulations

Once defined the stability criteria for the vehicle, it is possible to determine de maximum forces $\mathbf{F_S}$ and $\mathbf{M_S}$ that can be applied to the vehicle's center of mass for a specific situation. The forces can also be defined from the desired accelerations for the system. Either way, the problem consists in solving the following equation:

$$\begin{bmatrix} m\,a_x \\ m\,a_y \\ J_z\alpha_z \end{bmatrix} = \begin{bmatrix} \mathbf{F_S} \\ \mathbf{M_S} \end{bmatrix} + \begin{bmatrix} -mg\sin\theta \\ -mg\cos\theta \\ 0 \end{bmatrix} \tag{9}$$

where a_x, a_y e α_z are the desired accelerations in each axis, and the traction forces F_{T_f} and F_{T_r} are the variables.

Note that Eq. 11 has no unique solution and there is a set of combinations of traction forces on the front and rear wheels that can solve the equation. Therefore, the solution will be obtained from an optimization process whose objective is to maximize the stability of the vehicle, respecting the following restrictions:

1) $|F_{T_f}| \leq F_{T_{sat}}$, where $F_{T_{sat}}$ is the maximum traction force that the motor can produce, defined by the maximum torque of the motor divided by the radius of the wheel $F_{T_{sat}} = \tau_{max}/r$.
2) $|F_{T_r}| \leq F_{T_{sat}}$, where $F_{T_{sat}} = \tau_{max}/r$.
3) $N_f > 0$, to ensure that the front wheel does not lose contact with the ground.
4) $N_r > 0$, to ensure that the rear wheel does not lose contact with the ground.
5) $|F_{T_f}| \leq \mu N_f$, to ensure that there is no slippage in the front wheel.
6) $|F_{T_r}| \leq \mu N_r$, to ensure that there is no slippage in the rear wheel.

Once the optimization process determines the contact forces, the torque on each wheel is obtained by Eq. (10).

$$F_{T_r} = \tau_r/r, \;\; F_{T_f} = \tau_f/r \tag{10}$$

To validate the obtained equations and to analyze the best choice for the objective function of the optimization problem, several simulations were conducted in Matlab using the function *fmincon*. This function applies the interior-point optimization algorithm (Byrd et. al., 2000), which attempts to solve a sequence of approximate minimization problems including one slack variable on the objective function for each constraint of the problem and searching for the optimum point using a conjugate-gradient step.

The tests were conducted in several scenarios in which the vehicle is close to losing stability. Consider the two situations presented in Fig. 3. The first illustrates the vehicle moving on an inclined plane, where the contact angles of each wheel are the same as the inclination angle θ of the chassis. The second shows the vehicle passing through a bump and the contact angles of each wheel are different from each other.

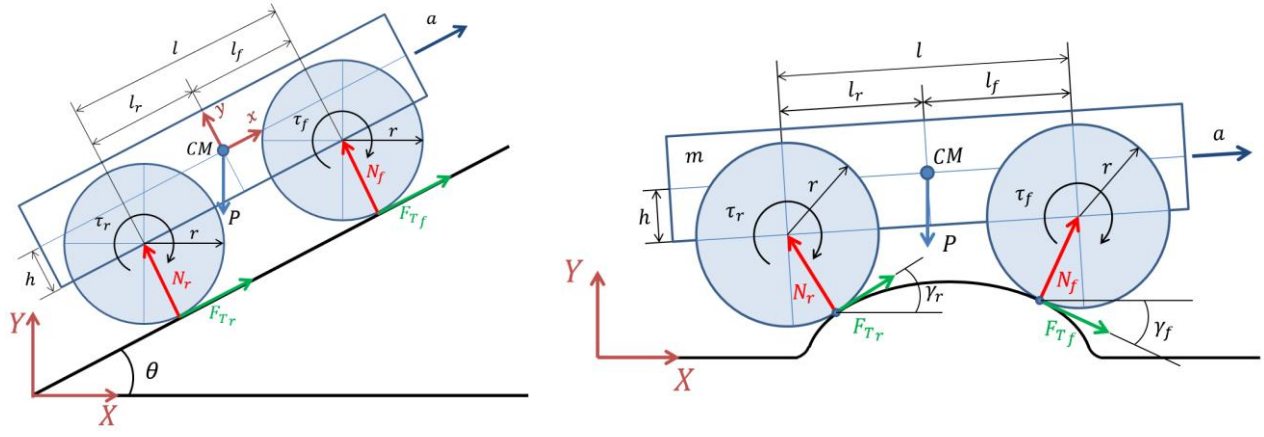

Figure 3 – Two different situations for a vehicle moving in uneven terrain

The vehicle parameters used in the simulations are presented in Tab. 1. During the simulations, the chassis inclination and the contact angles between the wheels and the ground were assumed to be known.

Table 1 – Parameters used in the simulations

Parameter	Symbol	Unit	Value
Vehicle mass	m	kg	*3.8*
Moment of inertia of the vehicle with respect to the z-axis	J_z	$kg.m^2$	*1.5*
Distance from front wheel to center of mass	l_d	m	*0.095*
Distance from rear wheel to center of mass	l_t	m	*0.095*
Distance between the wheels	$l = l_d + l_t$	m	*0.19*
Half of the height of the chassis center-of-mass	h	m	*0.0*
Wheel radius	r	m	*0.07*
Friction coefficient	μ	-	*0.5*
Maximum torque (motors)	T_{sat}	$N.m$	*0.88 (9 kgf.cm)*
Maximum traction force	F_{sat}	N	*12.57*
Gravity acceleration	g	m/s^2	*9.81*

For the movement on an inclined plane, the desired accelerations were set as a_x = 1.2 m/s^2, a_y = 0 m/s^2 and a_z = 0 m/s^2. The saturation torque of the motors is 0.88Nm and the objective function used was the absolute value of the difference between the front and rear normal forces. The objective here was to distribute the torques in a way that the normal forces would not be so different from each other and prevent the tipover. Considering a plane with 20 degrees inclination, the solution found was τ_f = 0.38Nm and τ_r = 0.83Nm. With these torques, the normal forces are N_f = 11.13N and N_r = 23.9N and there is no slippage. Increasing the inclination to 30 degrees, the solution is τ_f = 0.49Nm and τ_r = 0.88Nm, but the wheel slippage constraint could not be prevented. In the same situation, consider the objective is now to maximize the stability measure and therefore the accelerations are no longer input to the solver. The optimization algorithm converges to the amount of force necessary to keep the rover in the imminence of moving, which is expected, since that is the condition where the stability measure α reaches its higher value ($\beta_f = \beta_r$). The torques are τ_f = 0.32Nm and τ_r = 0.57Nm and the acceleration is zero. Figure 4 shows the forces acting on the rover in both optimizations processes: Fig. 4a shows the results for minimizing the normal difference between the wheels and Fig. 4b shows the results for maximization of the stability measure α.

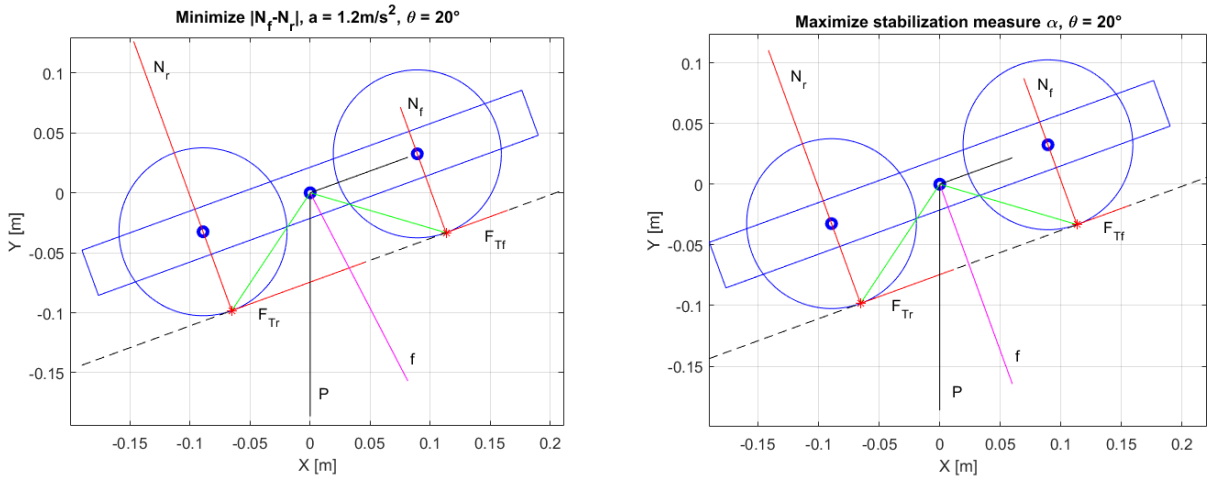

(a) **(b)**

Figure 4 – Results of the optimization in an inclined plane

In the second situation, in which the rover is passing through a bump, the desired accelerations were also set as a_x = 1.7 m/s^2, a_y = 0 m/s^2 and a_z = 0 m/s^2. The saturation torque remained the same and the objective was to minimize the absolute value of the difference between the front and rear normal forces. The angle θ was defined as 5° and the contact angles were set as $\gamma_f = -30°$ and $\gamma_r = 30°$. Tests were carried out with different chassis angles and different accelerations, as shown in Table 2.

Table 2 – Optimization results for torque distribution in uneven terrain

Conditions		Torques [Nm]		Normal Forces [N]	
Base angle [°]	Acceleration [m/s^2]	Front Wheel	Rear Wheel	Front Wheel	Rear Wheel
5	1.7	0.28	0.29	15.22	26.62
5	3	0.32	0.38	11.77	29.91
5	6	0.17	0.83	6.04	39.47
10	1.7	0.32	0.67	14.29	27.72
10	3	0.32	0.80	11.05	31.02

Figure 5a illustrates the forces for $\theta = 5°$ and $a_x = 3.0$ m/s^2 and Fig. 5b for $\theta = 10°$ and $a_x = 3$ m/s^2. For the case in which the base angle is 5°, slippage starts to happen after $a_x = 6.2$ m/s^2 approximately; and for base angle 10°, it is not possible to avoid slippage with accelerations higher than 3.5m/s^2.

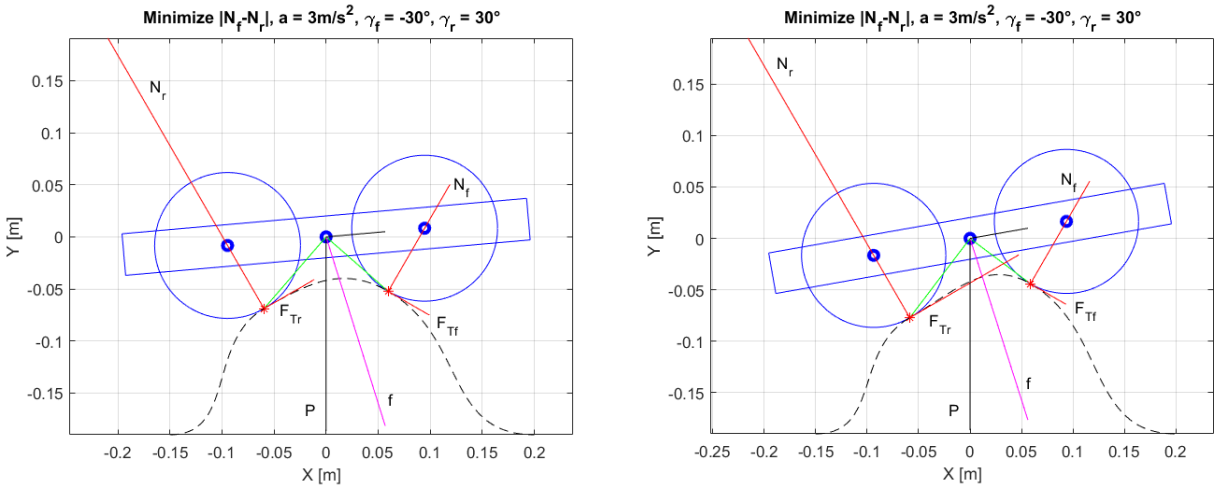

(a) **(b)**

Figure 5 – Results of the optimization on uneven terrain

The results obtained with the optimization show improvement of maneuverability in rough terrain and the computational cost of the algorithm developed is very low (mean of 0.09 seconds in a notebook with intel core i7 processor and 16GB of RAM). One problem with this approach is that the torque distribution results are sensitive to the initial solution supplied to the solver. In all these simulations the initial solution was half of the saturation torque on both wheels. However, if another initial solution is chosen, the solver may converge to a different local minimum and the results will be different. During the simulation tests, this initial point showed the best results.

Genetic Algorithm and Matlab Simulations

The evolutionary model used here is based on a multi-objective genetic algorithm. The multi-objective analyses is useful as it is possible to obtain even non-ideal solutions for the mechanical problem. The first objective, in this case, is similar to the anterior case: to obtain torques that can guarantee the stability according to the previously presented criterion. A second objective is established from the 5th and 6th restrictions. Now, the robot's wheels can slip, but this possibility must be minimized. This consideration is advantageous when dealing with high inclined terrains. In fact, when the slippage condition is a restriction, impossible solutions can appear to solve the dynamical problem.

The individuals of the algorithm are the torque in frontal and rear wheels, as the vehicle acceleration. The motor saturation and the contact with the ground continue being considered restrictions of the system. The computational simulations are based on an inclined plan and for different angles. The vehicle parameters are that presented in Table 1. Simulations were executed using the Matlab Optimization Toolbox, which is based on the NSGAII algorithm. The minimal number of 100 individuals and 1000 generations is sufficient to guarantee the obtaining of an optimal result. Elitism is used in 5% of the population and the crossover in 80% of the individuals. The Pareto fraction is set to 35% of them. The time of simulation is set to 2 seconds and the initial velocity is null.

For instance, by considering that the vehicle needs to climb a planar terrain with 40 degrees of inclination, the Pareto Frontier shown in Fig. 6 is generated. The optimization algorithm and the dynamical equations show that an acceleration of 0.26 m/s² and torques of 0.65 Nm in rear wheels and 0.08 Nm in frontal wheels guarantee the dynamical stability. However, the normal forces are almost zero in frontal wheels and slippage occurs. In fact, according to the Fig. 6, only one objective can categorically be achieved. The values generated by the genetic algorithm will be experimentally verified in this work.

For minor inclinations, the genetic algorithms generate better results. By considering a plane with 20 degrees of inclination, an optimal output of the algorithm is an acceleration of 0.34 m/s². The torques are $\tau_f = 0.17$ Nm and $\tau_r = 0.37$ Nm. With these torques, the normal forces are $N_f = 5.9$ N and $N_r = 11.6$ N. Slippage does not occur in this case. Moreover, the genetic algorithm gives the output information that accelerations until 2.2 m/s² guarantee the two objectives reaching. For a plane with 30 degrees of inclination, the optimal acceleration is reduced to 0.10 m/s². In this condition, the torques are $\tau_f = 0.16$ Nm and $\tau_r = 0.48$ Nm. The normal forces are $N_f = 4.5$ N and $N_r = 11.6$ N. Higher accelerations can produce slippage, as the normal forces can reaches values minor than 3 N. This result is qualitatively similar to the obtained results by the interior-point method.

The main advantage in use multi-objective genetic algorithms is that this technique provides a set of possible solutions for a dynamical problem. Each solution can be tested automatically, which offers to the robot a capacity of prediction of movements. The results obtained in the multi-objective can even be part of a database in the robot memory. However, the

main disadvantage is that genetic algorithms cannot be used online. Thus, the use of the two techniques adopted in this work is convenient in general applications with mobile robots.

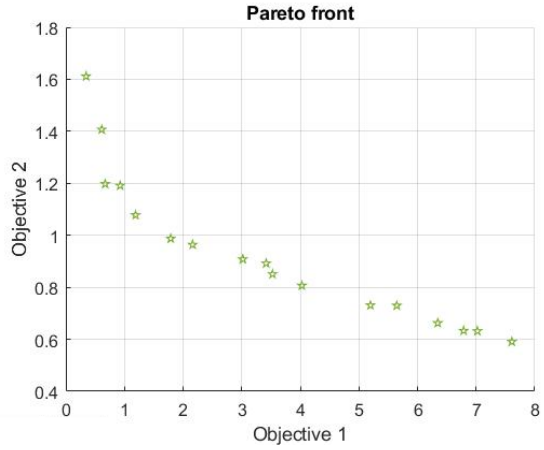

Figure 6 – Pareto frontier obtained in simulations, θ = 40°.

VEHICLE EXPERIMENTAL STABILITY TESTS

To verify the results given by the techniques explored in this work, experiments are performed on the four wheel drive mobile robot shown in Fig. 7. The robot has an electrical current feedback, used to estimate the torque at each wheel. The torque constant, which relates electrical current and mechanical torque, is $K_t = 0.18$. Tests are performed with the rover on a wooden ramp, which can be sloped at several angles. The desired accelerations are introduced in the system by means of velocity tuning.

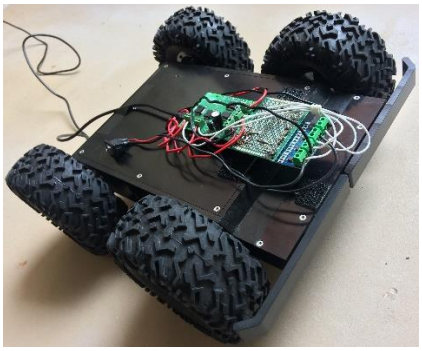

Figure 7 – Mobile robot used in experimental tests.

Initial tests are performed with the ramp at a 20 degree slope. Using the acceleration of 0.34 m/s², a value obtained with the genetic algorithm, the mean torques in Fig. 8 (a) are generated. According to the algorithm, the frontal wheels should present a torque of 0.17 Nm for the given situation. In fact, the experimental data confirms that this value is realistic. A peak appears in the first seconds of the experiment, related to the necessary torque to start the movement of the robot, and later a torque of 0.17 to 0.19 Nm is found sufficient for the ramp climbing. However, the torques at the rear wheels are discrepant to the simulated values. Similar results are obtained in tests on a plane with a 30 degree slope. The simulated torque at the frontal wheels is 0.16 Nm and the torque measured in the experiment is near 0.2 Nm, as shown in Fig. 8 (b). In this case, the acceleration is reduced to 0.10 m/s². Medium accelerations, between 0.10 and 1.4 m/s², might imply in slippage. Accelerations larger than 1.4 m/s² are impossible to be executed, because of the wheels' inertia. It is also possible to observe in the figures a variation in the torque signal. This reading is produced by the use of low-cost current sensors and by the friction between soil and wheels.

The problem related to the discrepancy between simulated and real torque at the rear wheels can be better visualized in higher slopes. The simulations are established considering that all the wheels start the movement at the same time. However, in real case applications, the frontal wheels, which have minor normal forces, start to move before the rear wheels. When the frontal wheels show this behavior, they support the rear wheels, which can start the movement with lower values of torque. This is a source of slippage and, consequently, loss of stability in the system.

To verify the influence of the frontal wheels in the beginning of the movement and validate the simulations for the rear wheels, a new test is implemented. Now, only the rear wheels are actuated. In this case, a ramp with a 30 degree slope is adopted. Figure 8 (c) shows the torque values oscillating between 0.30 and 0.45 Nm. These torques agree with

the value found in the genetic algorithm optimization, 0.37 Nm. The signal oscillations occur because, with only two-wheeled drive, the robot is not able to climb the ramp.

An extreme situation can also be tested, related to highly sloped terrains. Considering a terrain with a 46° slope, which is the maximum tested angle that the robot can climb, the expected acceleration generated by the genetic algorithm is 0.05 m/s². In this case, the simulated torque at the frontal wheel is 0.12 Nm and at the rear wheel 0.81 Nm. According to Fig. 8(d), the torque at the frontal wheels approach the value obtained from the algorithm. At the rear wheels, the same behavior happens as in the other cases: the frontal wheels start to move beforehand and the torque experimentally obtained is lower than in the simulations. In Fig. 8(d) it is also possible to observe the signal oscillations, which are a result of the slippage at the robot wheels.

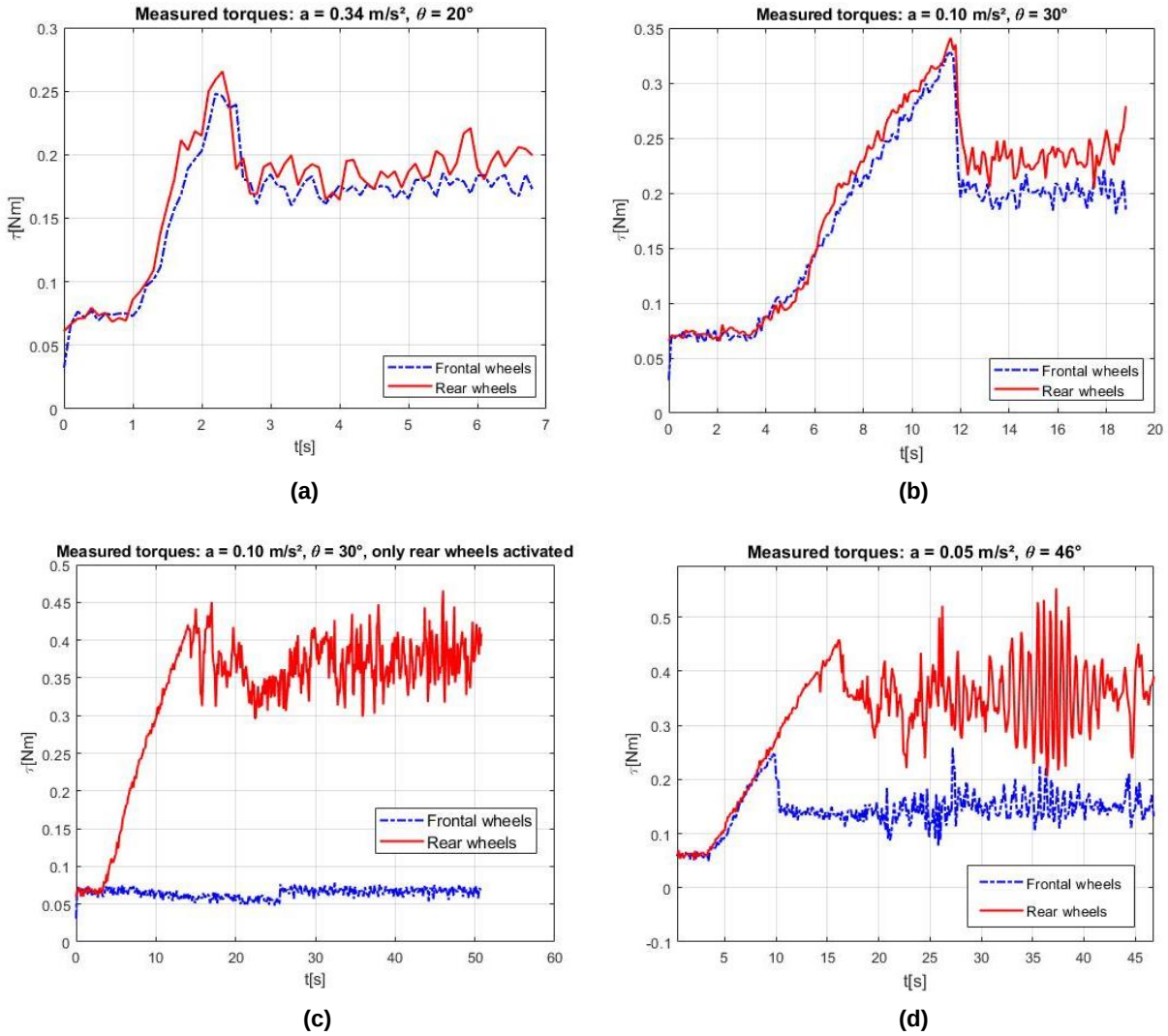

Figure 8 – Experimental torque measurement.

The presented results combine two techniques and an experimental evaluation for the problem of robot mobility in inclined terrains. The torque at the frontal wheels corresponds to the expected values. At the rear wheels, the results can be improved with an adequate torque control. Moreover, a larger set of values of acceleration might be tested in each inclination, to evaluate the algorithms. However, even when the stall torque is not reached, the inertia of the traction system does not allow elevated accelerations on an inclined terrain. Thus, some simulated accelerations could not be verified in the experiments.

CONCLUSIONS

In this work, two algorithms for torque optimization were implemented to control the mechanical stability of a mobile robot. The first, based on gradient optimization, was tested via Matlab simulations for a vehicle moving on flat inclined terrain and more challenging terrain, with different contact angles on the wheels. The second, based on genetic algorithms, was tested only for a robot moving on an inclined plane with both Matlab simulations and experimental tests using a mobile robot. Theoretical, numerical and experimental analyses show that the described methodology can improve the performance of autonomous vehicles moving in rough terrain. The main contributions of this paper are related to the algebraic methods that it describes and the simplified techniques of solution. In fact, algebraic approaches can be easily

generalized for other types of wheeled vehicles or other environmental conditions. Thus, this method is robust and with easy implementation for general purpose mobile and service robots, such as the ones used in agricultural, civil construction, rescue or even industrial applications. Future work includes further experimental tests in different conditions, more simulations in terrains with increasing roughness, and the establishment of a torque control technique for this kind of robot. Additionally, the model presented here will be adapted for 3D simulations including some dynamic effects.

ACKNOWLEDGMENTS

The authors would like to thank the institution CNPq and CAPES for the financial support to this research.

REFERENCES

Byrd, R. H., J. C. Gilbert, and J. Nocedal, 2000. “A Trust Region Method Based on Interior Point Techniques for Nonlinear Programming.” Mathematical Programming, Vol 89, No. 1, pp. 149–185.

Caltabiano, D., Ciancitto, D. and Muscato, G., 2004, Experimental Results on a Traction Control Algorithm for Mobile Robots in Volcano Environment, Proceedings of the IEEE International Conference on Robotics and Automation, New Orleans, pp. 4375-4380.

Hamid, A. A., Nazih, A., Ashraf, M. and Khamis, A., 2016, International Workshop on Recent Advances in Robotics and Sensor Technology for Humanitarian Demining and Counter-IEDs (RST), pp. 1-6.

Iagnemma, K., Rzepniewski, A., Dubowsky, S., Pirjanian, P., Huntsberger, T. and Schenker, P., 2000, Mobile Robot Kinematic Reconfigurability for Rough Terrain, Proc. SPIE, Sensor Fusion and Decentralized Control in Robotic Systems III, Vol. 4196.

Iagnemma, K. and Dubowsky, S., 2004, Traction Control of Wheeled Robotic Vehicles in Rough Terrain with Application to Planetary Rovers, The International Journal of Robotics Research, Vol. 23, No. 10–11, pp. 1029-1040.

Jin, X.-B., Su, T.-L., Kong, J.-L., Bai, Y.-T., Miao, B.-B. and Dou, C., 2018, State-of-the-Art Mobile Intelligence: Enabling Robots to Move Like Humans by Estimating Mobility with Artificial Intelligence. Applied Sciences, Vol. 8, No. 379.

Khamis, A., 2016, Minefield Mapping using Distributed Mobile Sensors, Proceedings of the International Conference on Robotics and Automation for Humanitarian Applications, Kerala, India, pp. 1-6.

Lamon, P. and Siegwart, R., 2005, Wheel Torque Control in Rough Terrain: Modeling and Simulation, Proceedings of the IEEE International Conference on Robotics and Automation, Barcelona, pp. 867-872.

Michaud, S., Gibbesch, A., Thueer, T., Krebs, A., Lee, C., Despont, B., Schaefer, B. and Slade, R., 2008, Development of the ExoMars Chassis and Locomotion Subsystem, Proceedings of the International Symposium on Artificial Intelligence, Robotics and Automation in Space (i-SAIRAS), Pasadena.

Papadopoulos, E. and Rey, D. A., 2000, The Force-Angle Measure of Tipover Stability Margin for Mobile Manipulator, Vehicle System Dynamics, Vol. 33, Issue 1, pp. 29–48.

Rasam, H. R., 2016, Review on Land-Based Wheeled Robots, International Scientific Conference Week of Science in SPbPU, Saint Petersburg, Vol. 53, No. 1058.

Silva, A.F.B., Santos, A.V., Meggiolaro, M.A. and Neto, M. S., 2010, A Rough Terrain Traction Control Technique for All-Wheel-Drive Mobile Robots, Journal of the Brazilian Society of Mechanical Sciences and Engineering, Vol. 32, No. 4, pp. 489-501.

Stückler, J., Schwarz, M., Schadler, M., Topalidou-Kyniazopoulou, A. and Behnke, S., 2016, NimbRo Explorer: Semiautonomous Exploration and Mobile Manipulation in Rough Terrain, Journal of Field Robotics, Vol. 33 Issue 4, pp. 411-430.

Xu, H., Liu, X., Fu, H., Putra, B. B. and He, L., 2014, Visual Contact Angle Estimation and Traction Control for Mobile Robot in Rough-Terrain, Journal Of Intelligent & Robotic Systems, Vol 74, Issue 3-4, pp. 985-997.

RESPONSIBILITY NOTICE

The authors are the only responsible for the printed material included in this paper.